Journal of
Materials Sciences and Applications

JScholar
Fostering Scholarly Communication

Research Article Open Access

Synthesis, Structural, Optical Properties and Toxicity Against Cancer Cells of New Urea-$Cdcl_2$ Complex

Férid Ben Nasr[1*], Hajer Guermazi[1], Sami Aifa[2], Samir Guermazi[1]

[1]Laboratory of Materials for Energy and Environment, and Modeling, University of Sfax, Faculty of Sciences of Sfax, Soukra road, Sfax, Tunisia
[2]Laboratory of Molecular and Cellular Screening Processes, Biotechnology center of Sfax, Sfax, Tunisia

***Corresponding authors:** Férid Ben Nasr, Laboratory of Materials for Energy and Environment, and Modeling, University of Sfax, Faculty of Sciences of Sfax, Soukra road, Km 3.5, B.P: 1171, 3000 Sfax, Tunisia, Tel: +216 74 276 400, Fax: +216 74 274 437, E-mail: fd.bennasr@gmail.com

Received Date: January 06, 2021 **Accepted Date:** February 06, 2021 **Published Date:** February 08, 2021

Citation: Férid Ben Nasr (2021) Synthesis, structural, optical properties and toxicity against cancer cells of new Urea-CdCl2 complex. J Mater sci Appl 5: 1-12.

Abstract

The present study, deals with the investigation of new synthesized Urea-$CdCl_2$ complex [$(NH_2CONH_2)CdCl_2$] properties at room temperature. X-ray diffraction (XRD), infrared (IR), UV visible (UV-vis), photoluminescence (PL) measurements are carried out to characterize structural and optical properties. The toxicity of this complex was tested as well.

The obtained results confirmed the formula $(NH_2CONH_2)CdCl_2$ for the formed complex, in full agreement with the literature data.

XRD indicates that this compound crystallizes at room temperature in the triclinic system with space group. The average crystallite size estimated from Debye Scherrer model was found to be about 61 nm. IR spectrum confirmed the presence of the organic chains of the Urea-$CdCl_2$ complex. Furthermore, it proved that the cohesion between the organic and inorganic groups is insured by the Cd-O bonds.

Besides, the optical properties were examined by UV-vis and PL spectrocopies. The UV-vis absorption measurements showed that the optical absorbance is higher in the Ultraviolet ($\lambda < 300$ nm) domain. The optical band gap (E_g) is deduced to be 4.02 eV. Optical parameters were estimated from the absorption data. Moreover, the toxicity of the Urea-$CdCl_2$ Complex was tested against normal kidney cell line (HEK293) and two cancers cell lines (MDA and T47D). The obtained results showed that Urea-$CdCl_2$ improved the toxicity against the breast cancer line T47D.

Keywords: Urea Complex; Defects; Absorption; Toxicity

Introduction

In today's world the arrangement of two organic and inorganic phases is refined by the formation of a new material called hybrid material. The notion of organic / inorganic hybrid materials has the possibility of being able to combine, within the same compound, the initial properties of the organic constituents (solubility and flexibility) and inorganic properties (ferroelectricity, ferroelasticity, frequency doubling, electronic and optical properties, magnetic). The combination of the respective properties allows to consider very varied applications, described later, in several fields: industrial [1,2], environmental [3], medical [4,5], agricultural [6] biological and biochemical [7,8] and therapeutic [9,10].

Hybrid materials are the subject of much research, both fundamental and applied [11-16]. These works deal in general with the study of the change of the properties of the hybrids notably mechanics [17] thermal [18-21] electrical [22] and magnetic [23] compared to those of the pure organic polymers.

These hybrid compounds constitute, in fact, a very important crystalline class which has gained a great interest during these last decades. Indeed, the interesting optical and electrical properties exhibited by materials with the potential for simple and inexpensive synthesis techniques give them great interest in the fabrication of optoelectronic devices such as light emitting diode, field effect transistors and photovoltaic cells.

Metal-urea complexes are known as chemically stable compounds. Urea complexes with metal ions are used as fertilizer [24,25]. Some metal-urea complexes have a pharmaceutical application, for example the Latin-urea complex, which is used as anti-tumor [25,26].

The metal-urea complexes are water-soluble powders of different colors depending on the used metal salt.

Urea (NH_2CONH_2) is one of the organic nonlinear optical (NLO) materials which have been first adopted for NLO devices [27]. It is synthesized in the liver by the combination of two molecules of ammonia (NH_3) with a molecule of CO_2 in the urea cycle.

In this work, our aim is to synthesize a new hybrid material with good structural and optical properties for photovoltaic cell applications. As well as studying the influence of this new metal cation on physicochemical and optical properties. The toxicity of the new Urea-$CdCl_2$ complex was tested as well.

Experimental

Synthesis of materials

Urea, $CdCl_2$ and distilled water solvent were obtained from Aldrich Company. All chemicals used in this study were of analytical grade and they were used without further purification.

The studied compound was synthesized by slow evaporation at room temperature of aqueous solution. This method is based on chemical reactions between raw materials (NH_2CONH_2 and $CdCl_2$ of high purity), at ambient conditions, according to the following equation: (NH_2CONH_2) + $CdCl_2$ (NH_2CONH_2)$CdCl_2$

The synthesis is carried out at room temperature as follows: In a first beaker powder of urea is dissolved in distilled water, the solution is stirred with a magnetic stirrer for 5 minutes, a solution aqueous cadmium chloride ($CdCl_2$) is then added to the solution of the urea with a few drops of HCl keeping stirring until complete dissolution. The final solution is then allowed to evaporate at ambient conditions. Since the day of preparation, the solution is constantly monitored until the first crystals are obtained.

Characterization methods

X-ray powder diffraction was obtained using Bruker D8Advance X-Ray diffractometer with monochromated CoKα1 radiation (λ=1.789 Å). Micro-structural parameters such as the crystallite size, the strain, the dislocation density, are computed.

Then infrared spectra of the samples were recorded in the spectral range 4000 – 400 cm-1 using a Nicolet 5ZDX Fourier transforms spectrometer.

Optical absorptiona measurements were done at room temperature using a UV–vis–NIR spectrophotometer (Optizen POP) in the wavelength range of 200 – 950 nm.

In order to know the luminescent behavior of the Urea-$CdCl_2$ crystal, a PL spectrum was recorded using a JOBIN YVON HR320 spectrometer under ambient conditions, with an excitation wavelength of 375 nm.

Toxicity test

Cell Culture

Two cancer cell lines belonging to Human Breast Adeno carcinoma were used throughout this study: T47D (estrogen receptor positive) and MDA-MB-231 (estrogen receptor negative), in addition to the non-tumor cell line of human embryonic kidney cells (HEK 293).

HEK293 and MDA-MB-231 cell lines were grown in DMEM while T47D cells were maintained in RPMI supplemented with 10% foetal bovine serum, 50 IU/ml penicillin, 50 mg/ml streptomycin at 37 °C in a humidified 5% CO_2 atmosphere.

Measurement of Cell Viability

Cells were plated in 96-well plates at a density of 80.000 cells /ml, permitted to adhere for 24h, before the treatment by increasing concentrations of each compound added to culture medium. After 48h the media were removed and MTT solution (5mg/ml) was added to each well containing 100 µl fresh medium.

After 4h of incubation, the medium was removed and replaced by 100 µl of SDS 10% in order to dissolve the formazan precipitate. The absorbance was measured in an ELISA reader (Thermo Varioskan) at 570 nm. The cell viability ratio was calculated by the following formula: Cell viability ratio (%) = ($OD_{treated}/OD_{control}$) ×100%.

Cytotoxicity was expressed as the concentration of each compound inhibiting cell growth by 50% (IC50 value).

Results and discussion

Microstructural properties

To check the crystallinity and crystal phases of the prepared powders, the XRD pattern has been performed and the results are shown in Figure 1.

We found that this compound is the cadmium chloride carbamide of chemical formula $(NH_2CONH_2)CdCl_2$ (Urea-$CdCl_2$) according to the map (ICSD # 039960) [28]. It belongs to triclinic system with the space group $P\bar{1}$. No other peaks related to impurities are observed, which proves the absence of any secondary impurity.

From XRD pattern, the lattice parameters a, b, c, α, β and γ as well as the volume (V) of the unit cell for triclinic system is calculated by using Eq.(1) and Eq.(2).The obtained values were given in Table 1.

Table 1: Lattice parameters and unit cell volume of Urea-$CdCl_2$ nanocrystals

a (Å)	b (Å)	c (Å)	α (°)	β (°)	γ (°)	V(Å3)	Z
3.77(8)	8.12(5)	10.05(1)	74.80(0)	81.77(0)	81.87(0)	292.87	2

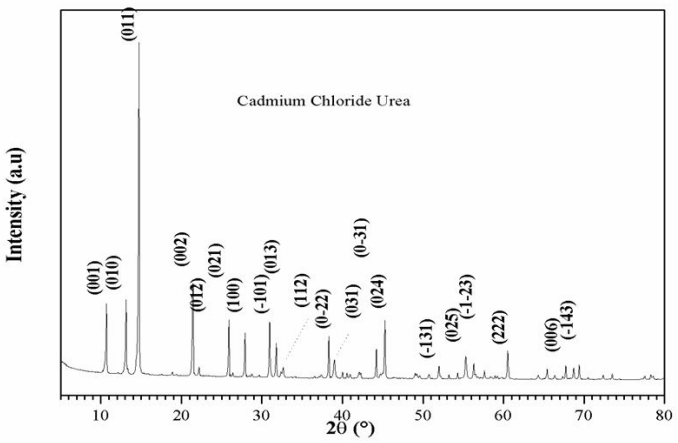

Figure 1: XRD pattern of the Urea-$CdCl_2$ powder

In order to investigate preferential orientation of crystallite in Urea-$CdCl_2$ compound, the texture coefficient TC(*hkl*) was evaluated for prominent diffraction peaks using the Eq. (3) [29].The values of TC(*hkl*) are plotted in Figure 2.

As shown in figure 2, the crystallites have a preferential orientation according to (024) direction.

The stacking fault is a planar imperfection that arises from the stacking of one atomic plane out of sequence with another while the lattice on either side of the fault is perfect. The presence of a stacking fault gives rise to a shift in the peak positions observed relative to the ideal (ICSD # 039960) of Urea-$CdCl_2$. From XRD patterns, the peak shift Δ(2θ) for the oriented (*hkl*) planes was measured.

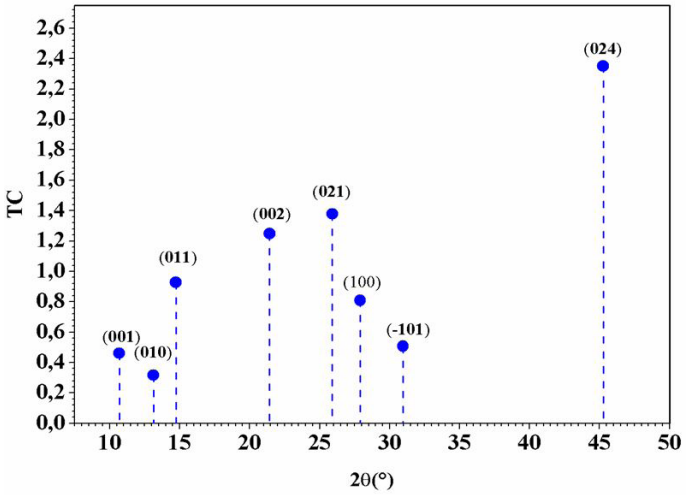

Figure 2: Evolution of texture coefficient (*TC*) for the prominent diffraction peaks

The stacking fault probability γ was calculated using Eq. (4) [30]. The obtained values were added in Table 2.

Table 2: The stacking fault probability values.

2 θ (°)		*hkℓ*	Stacking fault probability γ
(Measured)	(ICSD # 039960)		
10 .68	10.64	001	0.09(8)
13.12	13.18	010	0.13(5)
14.73	14.77	011	0.08(2)
21.43	21.39	002	0.05(3)
25.90	26.05	021	0.16(2)
27.89	27.90	100	0.00(5)
30.96	31.09	-101	0.11(8)
45.26	45.31	024	0.03(1)

The average crystallite size of the prepared compounds is estimated from the measured width of their XRD patterns by using Debye - Scherrer's formula: Eq (5) [31].

The dislocation density δ of Urea-$CdCl_2$ powder was calculated from Eq. (6) [32].

The values of the average crystallite size and strain were estimated to be about 61 nm and 2.67. 10^{-4} nm^{-2}, respectively.

FTIR analysis

The bands observed around 3476, 3443 cm^{-1} in the infrared spectrum are attributed to the asymmetric elongation vibration NH, while the bands observed around 3376, 3347, 3272, 3222 , 3125 are attributed to the symmetrical elongation vibration NH.

The NH_2 deformation and CO elongation modes are present at the 1667 and 1634 cm^{-1} bands [33-36].

The bands observed around 1615 and 1143 cm^{-1} are attributed to a NH_2 deformation vibration.

The peaks which appear around 1588 and 1478 cm^{-1} are attributed by stretching C = O and C-N respectively. We also note the presence of a symmetrical elongation vibration C-N at the level of the band 1019 cm^{-1}. The band at 760 cm^{-1} is attributed to a vibration of symmetrical deformation of O-C-O group and a deformation out of the plane (torsion) of ONCN group.

The bands observed around 671 and 610 cm^{-1} is attributed to a vibration of elongation C-O in the plan. We also note the presence of vibration modes of N-C-N deformation and NH_2 torsion around 534 and 494 cm^{-1}.

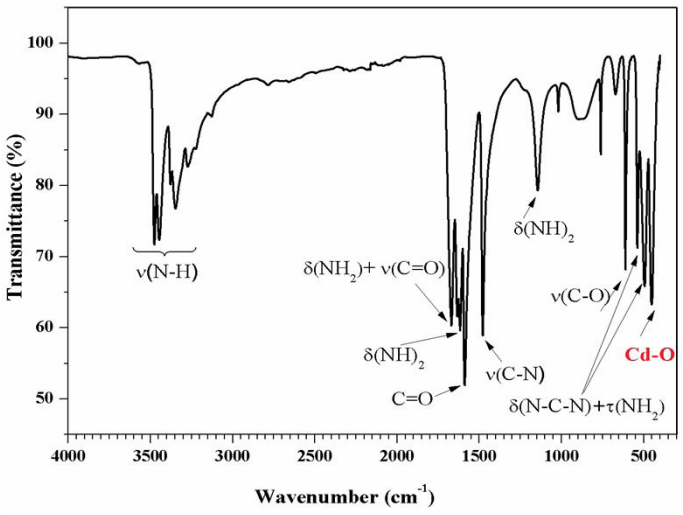

Figure 3: FTIR spectrum of Urea-$CdCl_2$ sample

The band observed around 449 cm^{-1} is attributed to a mode vibration of Cd-O. Finally, according to the reference [36], we can confirm the presence of the organic chain of our hybrid compound Urea-$CdCl_2$ and the cohesion between the organic chain and the inorganic part is ensured by the Cd-O bond (see Figure 4).

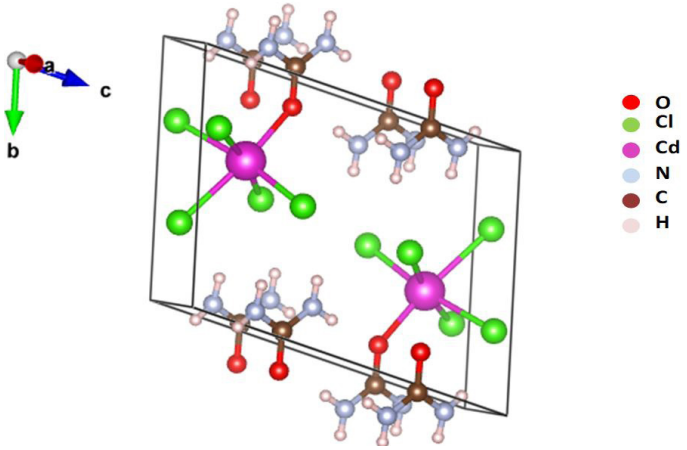

Figure 4: Structure of Urea-$CdCl_2$ [28]

Optical properties

The optical properties of the synthesized Urea-$CdCl_2$ complex were studied by UV–vis spectroscopy. The absorption, reflection and transmittance spectra of Urea-$CdCl_2$ compound against wavelength are shown in Figure 5.

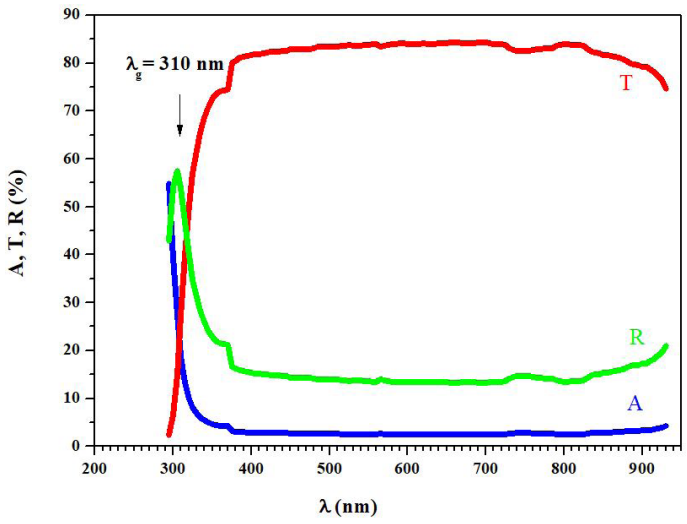

Figure 5: Absorption, transmission and reflection spectra of Urea-$CdCl_2$ complex

The spectra that the Urea-$CdCl_2$ complex exhibit high absorption in UV - range, and good transparency in the visible wavelength range.

There are two regions: a first region, that of strong transparency (λ > 375 nm). We show that the transmission is around 80 %.

This gives transparency in the visible and near infrared, properties recommended for applications as transparent electrodes.

A second region, that of high absorbance, corresponds to the fundamental absorption (λ < 375 nm) in the sample. The absorbance exhibits a decrease in the near IR region (around 820

nm). This shows that this compound can be used as optical filters in the ultraviolet. This absorption is due to the electronic band-to-band transition (from the valence band to the conduction band).

The absorption and extinction coefficients: The absorption coefficient α was calculated using Eq. (7) [37].

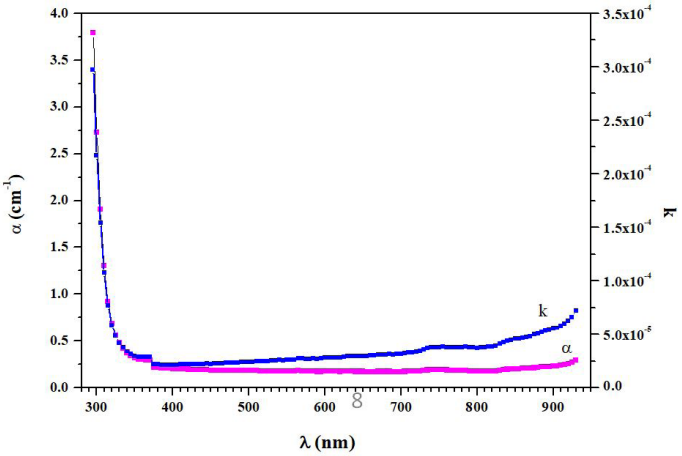

Figure 6: Variation of absorption coefficient (α) and extinction coefficient (k) of the sample as a function of wavelength

Variation of absorption coefficient (α) and extinction coefficient (k) of the sample as a function of wavelength as show in figure 6.

From Figure 6, (α) tends to decrease as the wavelength increases and is strongly dependent on the wavelength in the UV, but it remains substantially constant in the visible and near infrared range (400 - 750 nm). This behavior was observed for many compounds and can occur for many reasons, such as internal electric fields within the crystal, deformation of lattice due to strain caused by imperfection and inelastic scattering of charge carriers by phonons [38].

Around 820 nm, (α) increases to reach a maximum around 930 nm, then decreases again.

The extinction coefficient (k) follows the same evolution as (α). The small values of (k) in the (400 – 700) nm range explain the transparency of the compound.

A weak dispersion and it remains substantially constant in the visible region. The evolution of the refractive index of optical materials is very important for many applications such as optical glass.

Optical band-gap

The optical band gap E_g of synthesized complex is computed according to the Eq. (8) [39]. The usual method for determining E_g involves plotting $(\alpha h\upsilon)^{\frac{1}{n}}$ vs. photon energy (hυ). Figures 7 and 8 show the variation of $(\alpha h\upsilon)^{\frac{1}{n}}$ vs. hυ for Urea-$CdCl_2$ nanoparticles with n values of 1/2 and 2 respectively.

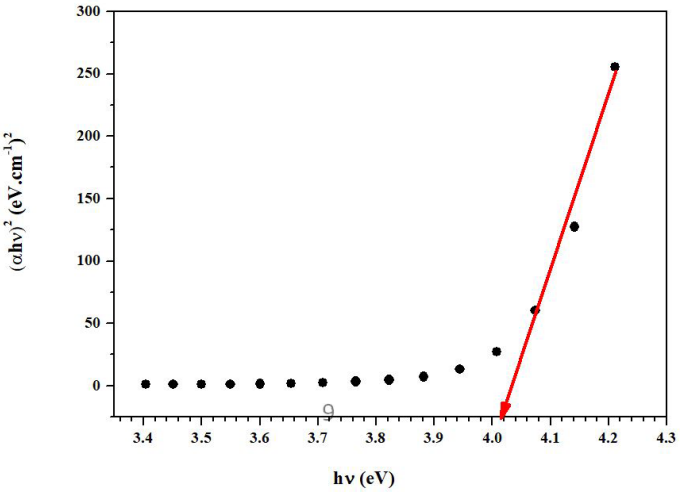

Figure 7: Plot of $(\alpha h\upsilon)^2$ vs. photon energy for the Urea-$CdCl_2$ sample

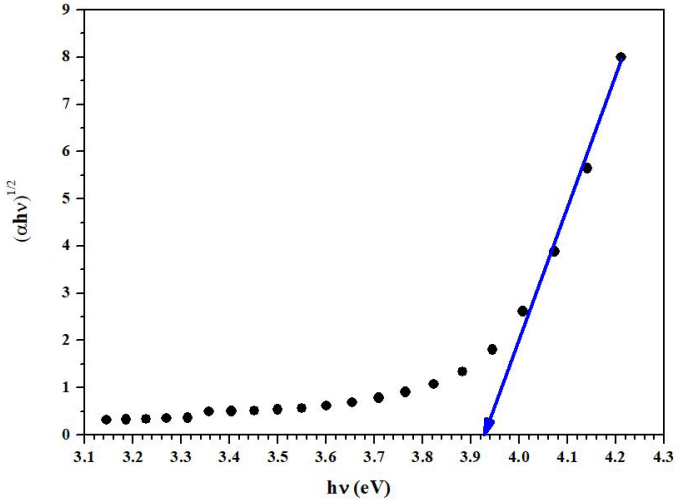

Figure 8: Plot of $(\alpha h\upsilon)^{\frac{1}{2}}$ vs. photon energy for the Urea-Cd sample

The values of direct and indirect band gap for the Urea-$CdCl_2$ sample are 4.02 eV and 3.96 eV respectively. These high values demonstrate non-conductive properties of this complex.

Urbach energy

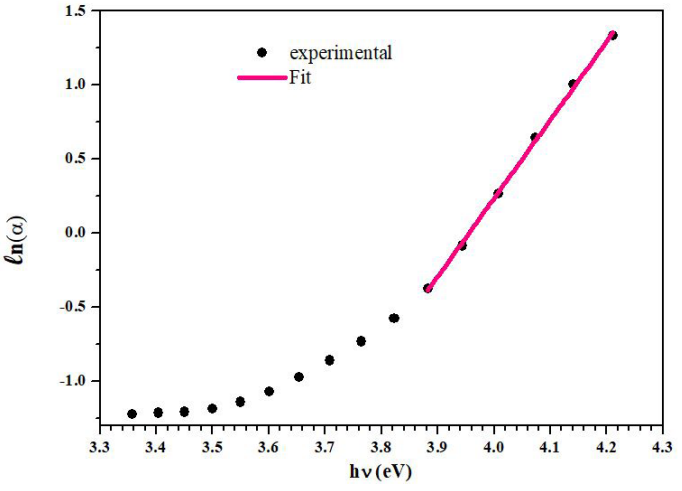

Figure 9: ln(α) versus energy (hν)

The Urbach energy characterizes local defects which create localized states in the band gap. In fact the presence of defects in the compound often reveals the formation of band tailing in the band gap, the interactions with phonons and the presence of a tail absorption profile which follows the empirical Urbach laws (Eqs.9 and 10) [40,41] as seen in Figure 9.

The width of located states (band tail energy or Urbach energy E_u) is estimated from the slope of ln(α) versus energy (hν) (Figure 9). The estimated E_u value is equal to 189 meV. The found value of E_u is low compared to that in the case of hybrid perovskites [13,14].

Refractive index

Firstly, the refractive index n of the sample is calculated from the gap energy by using the Eq. (12) [42]. The simplification of Eq. (12) leads to Eq. (13). The value of the refractive index n is found to be 2.17.

The dispersive behavior of the refractive index n(λ) was deduced from absorption data using the Eq. (14).

Figure 10 shows the evolution of the refractive index of the Urea-$CdCl_2$ complex. The refractive index of the sample decreases in the UV range and it remains substantially constant in the visible region (400 - 800 nm). Moreover, n increases in near infrared (NIR) region (around 820 nm). Thus, Urea-$CdCl_2$ compound blocks a selective NIR wavelength.

In UV range n reaches a high value, which makes this compound suitable for UV – blocker devices.

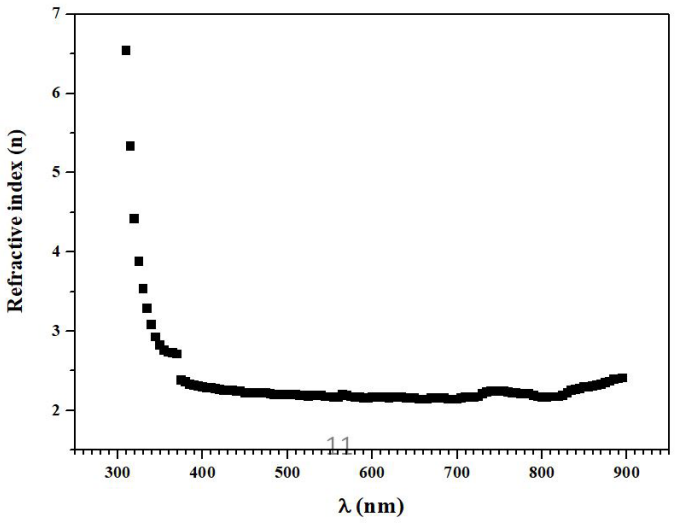

Figure 10: Plot of the refractive index vs. wavelength

We have also calculated some other optical constants based on Wemple– DiDomenico (WD) single oscillator model using Eq (15) [43,44]. This model uses a single-oscillator description of the frequency dependent dielectric constant to define dispersion energy parameters E_0 and E_d. E_0 is the energy of the effective dispersion oscillator and E_d is the dispersion energy, is a measure of the average strength of the inter-band optical transitions.

The dispersion plays an important role in the research for optical materials because it is a significant factor in optical communication and in designing devices for spectral dispersion.

The relation between the refractive index n and the single oscillator strength below the band gap is given by Eq. (16) [45].

The WD model is used to fit the experimental data of Figure 11. This model uses a single-oscillator description of the frequency dependent dielectric constant to define dispersion energy parameters E_0 and Ed. E_0 is the energy of the effective dispersion oscillator and E_d is the dispersion energy, is a measure of the average strength of the interband optical transitions. E_0 and E_d can be determined from the intercept,$(\frac{E_o}{E_d})$ and the slope $(-\frac{1}{E_o E_d})$.

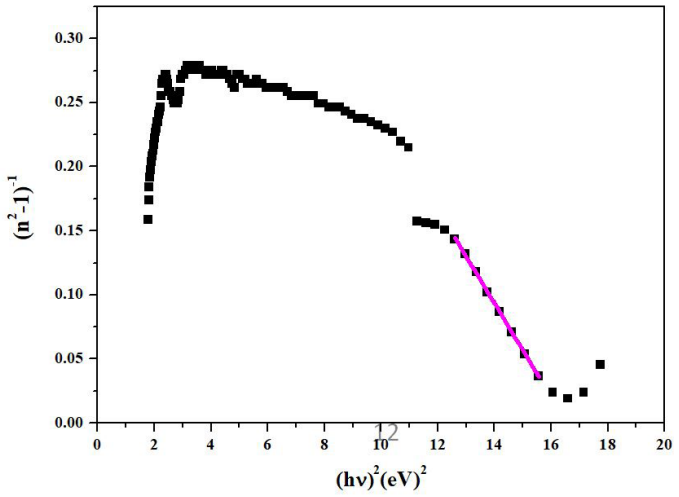

Figure 11: Plots of $(n^2-1)^{-1}$ vs (eV)²

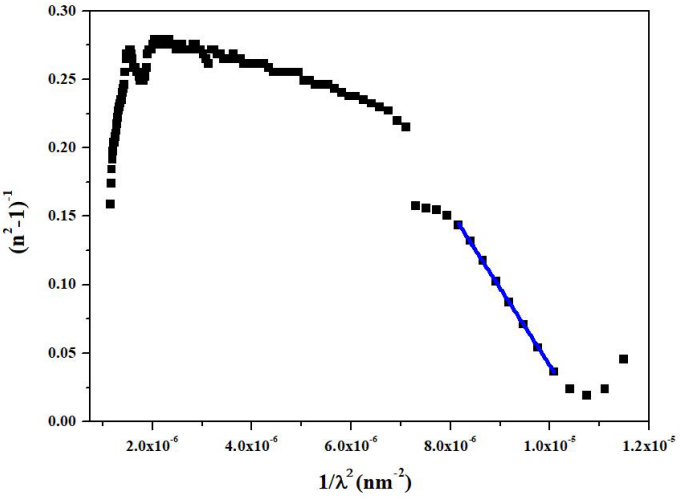

Figure 12: Plots of $(n^2-1)^{-1}$ vs $(\frac{1}{\lambda^2})$

Table 3: Calculated values of parameters E_0, E_d, λ_0, S_0 and n_∞

parameters	E_0(eV)	E_d(eV)	λ_0(μm)	S_0 (μm^{-2})	n_∞
Urea-$CdCl_2$	4.07	6.72	0.30	17.71	1.62

Under the same model, the refractive index can also be analyzed to determine the high wavelength refractive index n_∞, the average oscillator wavelength λ_0 and the oscillator length strength S_0. These values can be obtained by using the Eq. (16), Eq. (17) and Eq. (18) respectively. By fitting the plots of $(n^2-1)^{-1}$ vs $\frac{1}{\lambda^2}$ (Figure 12), we can deduce the values of λ_0 and S_0. E_0, E_d, λ_0 and S_0 are gathered in Table 3.

Optical dielectric constant

The complex dielectric constant given by Eq. (19) characterizes the optical properties of the solid material. The real part of the dielectric constant shows how much it wills lowdown the speed of light in the material, whereas the imaginary part shows how much a dielectric material absorbs energy from an electric field due to the dipole motion. The real and imaginary parts of dielectric constant for the two samples are also determined by the following relations (Eq.19) [46].

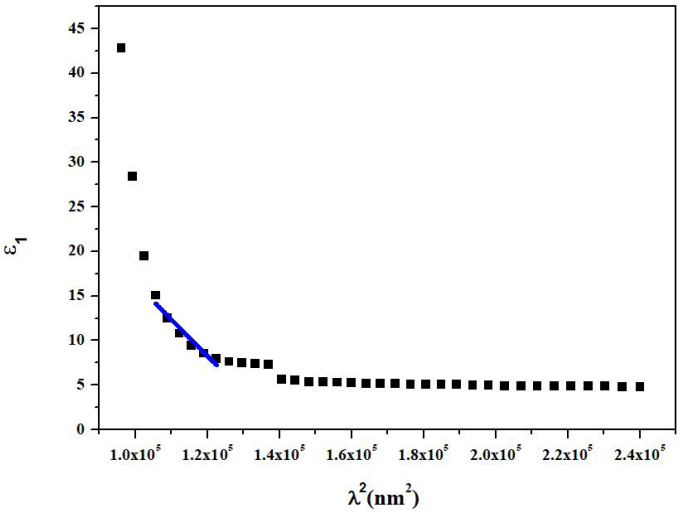

Figure 13: ε_1 vs λ^2

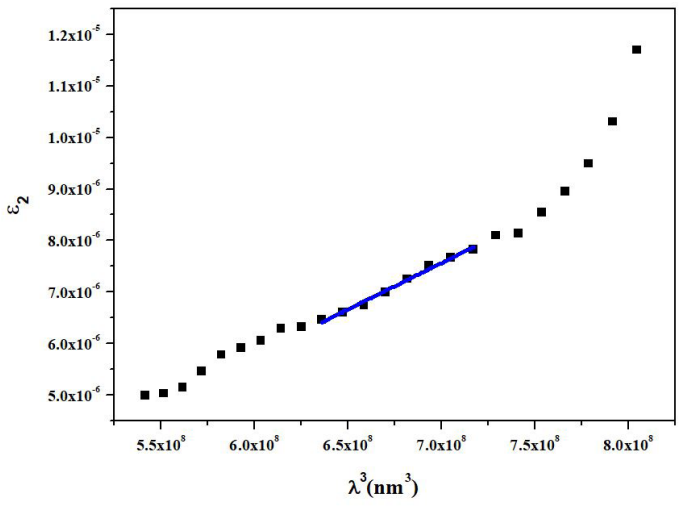

Figure 14: ε_2 vs λ^3

For the sample, in infrared domain, it is found that ε_1 is a linear function of the square of the wavelength (Figure 13), while ε_2 is linear with λ^3(Figure 14).

These results can be used in order to determine the optical constants: ε_∞, ω_p and τ which, respectively, represent the dielectric constant at high frequencies, the plasma pulse and relaxation time. These parameters can be determined from the equations Eq. 20 [47,48].

We can also calculate the values of the optical conductivity given by Eq.21 [49,50]. The calculated values of these constants are gathered in Table 4.

Table 4: Calculated values of ε_∞, w_p, and other constants

parameters	ε_∞	wp (10^{15} rads^{-1})	τ (10^{-8}s)	N/m* (10^{49}g^{-1}cm^{-3})	σ(S.cm-1)
Urea-$CdCl_2$	5.71	5.03	1.21	4.00	12400

Photoluminescence

PL study is a powerful tool to investigate the optical properties of Urea metal complex. The recorded spectrum is shown in Fig. 15. This analysis will give important information about the absorption and emission of light.

The PL spectrum of the Urea-$CdCl_2$ complex shows a broad emission band located at around 480 nm (2.588 eV), which is consistent with absorption measurement. This emission band is spread over the visible domain. In order to further attribution of the origin of these large white emissions, we proceeded to a decomposition of the broad PL band.

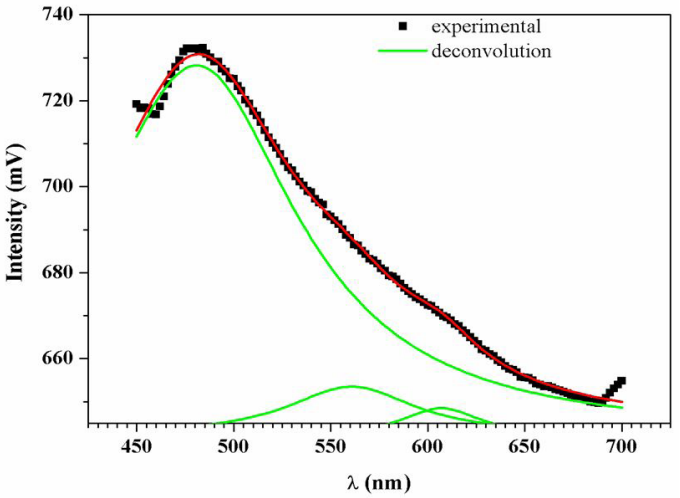

Figure 15: Photoluminescence spectrum of Urea-$CdCl_2$ sample

The peak around 480 nm was observed by Kanika Thukral, *et al.* [51] in $(C_5H_9NO_2)CdCl_2 \bullet H_2O$ compound. This compound has the same inorganic part ($CdCl_2$) as the present Urea-$CdCl_2$ complex, which proves that this emission is related to this common part. The width of this peak is linked

to a wide distribution of defects in the band gap, in accordance with the high band gap energy deduced from absorbance data. Furthermore, PL emission around 606 nm was related to the presence of Urea group [52]. While, the main blue emission peak at 482 nm is generally attributed to the radiative recombination of a photogenerated hole with an electron occupying the oxygen vacancy. This peak is attributed to the excitonic transitions which are size-dependent and excitation wavelength independent of the certain wavelength range [53]. The green emission peak at 560 nm might have originated from the electronic transitions of ionized oxygen vacancies from the deep level donor to the valence band [54].

Toxicity test

We have studied the toxicity of the Urea-$CdCl_2$ Complex towards a normal kidney cell line (HEK293) and two cancer cell lines (MDA and T47D). Cells were treated with different concentrations ranging from 0.3 to 100 µM of the compounds during 48 h. Cell viability was evaluated by MTT assay as detailed in materials and methods.

We therefore determined the IC50 (inhibitory concentration of 50% of cells) in micromolar.

The obtained results showed that the viability of the used cell lines was reduced in a dose and compound-dependent manner with specific IC50 values (Table 5).

As expected, $CdCl_2$ is toxic to normal cells but cancer cells are more resistant. Although urea is not toxic but, when complexed with $CdCl_2$, it accentuates the toxicity towards normal cells (HEK293). Urea-$CdCl_2$ improved the toxicity against the breast cancer line T47. These finding could use the incorporation of $CdCl_2$ in organic compounds in order to create a tumour- specific toxicity. In fact a selective cytoxicity against cancer cell lines was obtained with chromium present in some arene tricarbonylchromium compounds vs the high toxicity of chromium in $K_2Cr_2O_7$ [55].

Table 5: The viability of the used cell lines with specific IC50 values.

	$CdCl_2$, H_2O	Urea	Urea-$CdCl_2$ complex
HEK293	2.54	> 100	2.01
MDA	78.19	> 100	61.6
T47D	36.73	77.83	72.92

Conclusion

Urea-$CdCl_2$ nanoparticles have been synthesized by evaporation method at room temperature. The prepared compound was characterized by XRD, FTIR, U.V–Vis and PL spectroscopy.

This compound is crystallized in the triclinic system with space group. The lattice parameters a, b and c are 3.77 Å, 8.12 Å and 10.05Å respectively.

The IR study show the presence of the organic chain of our hybrid compound Urea-$CdCl_2$ and the cohesion between the organic chain and the inorganic part is ensured by the Cd-O bond.

The measured optical band gap for Urea-$CdCl_2$ is 4.02 eV is in good agreement with literature.

The dispersion of the sample was studied using the Wemple–DiDomenico method. The oscillator energy E0 and the dispersion energy E_d was deduced: 4.07 and 6.72 eV respectively.

The spectra that the Urea-$CdCl_2$ sample exhibit high absorption in UV- range, and good transparency in the visible wavelength range. This shows that this compound can be used as optical filters in the ultraviolet.

From the PL study, one can see suggests that the material is a good candidate for blue light emission and has less defects.

The toxicity test technical results are showing that the viability of the used cell lines was reduced in a dose and compound-dependent manner with specific IC50 values. As expected, $CdCl_2$ is toxic to normal cells but causing less mortality on cancer cells. Even when complexed with urea (not toxic), $CdCl_2$ preserves its toxicity which accentuates against normal cells (HEK293). Meanwhile, Urea-$CdCl_2$ improved the toxicity against the breast cancer line T47D. These finding could use the incorporation of $CdCl_2$ in organic compounds in order to create a tumour- specific toxicity.

Acknowledgements

Authors gratefully thank the financial support of the Tunisian Ministry of High Education and Scientific Research. They appreciate the assistance of Prof. Y. Abid, Laboratory of applied physics, Faculty of Sciences of Sfax, for PL measurements and Prof H. Boughzala, Laboratory of Materials and Crystal-chemistry, University of Tunis El-Manar, Faculty of Science Tunis for XRD measurements.

References

1. M Bluthe (1986) Chemical news 44.

2. JP Pothet (2008) Checklist-packing materials 432.

3. T Ait-Hamouda et MJ (1981) Schwing-well, Analusis. 9: 93.

4. FW Wehrli, D Shaw, JB Kneeland (1988) Biomédical Magnetic Resonance Imaging, VCH, New York.

5. RB Lauffer, AC Vincent, S Padmanabhan, A Vilringer, S Sarni, et al. (1987) Hepatobiliary MR contrast agents: 5-substituted iron-EHPG derivatives Mag Res Med 4: 582.

6. S Grand, G Ferreti, JF Le Bas, H Mollier, M Vidal (1991) Vincens, Innov. Tech. Med.12, (1991) 295.

7. JL Pierre (1992) Fontecave, Chemical news, July-August 297.

8. C Dietrich-Buchecher, JP Sauvage (1989) Chemical news 139.

9. M Jaquinod, E Leize, K Klarskov, G Hegg, N Potier (1993) Dorsselaer, Analusis 21: 275.

10. D Comboli, J Besançon (1985) Chemical news. 53: 61.

11. L Rozes, N Steunou, G Fornasieri, C Sanchez (2006) Monthly magazine for chemistry. 137: 501.

12. C Sanchez, C Boissiere, D Grosso, C Laberty, L Nicole (2008) Chemistry of Materials. 20: 682.

13. R Lefi, F Ben Nasr, H Hrichi, H Guermazi (2016) optics 127: 5534–41.

14. R. Lefi, F Ben Nasr, H Guermazi (2017) Structural, optical properties and characterization of (C2H5NH3)2CdCl4, (C2H5NH3)2CuCl4 and (C2H5NH3)2Cd0.5Cu0.5Cl4 compounds. J Alloys Compounds 696: 1244-54.

15. R Lefi, Wissal Jilani, F Ben Nasr, M Kahlaoui, H Guermazi (2018) Synthesis, phase transition and analysis of high temperature AC conductivity of (C 2 H 5 NH 3) 2 Cd 0.5 Cu 0.5 Cl 4 perovskite 200: 12-8.

16. F. Ben Nasr, R. Lefi, H. Guermazi (2018) Analysis of high temperature phase transitions of copper doped (C2H5NH3)2CdCl4 perovskite. J molecular structure 1165: 236-45.

17. Okada A, Usuki A (1995) The chemistry of polymer-clay hybrids. Mater Sci Engng C3: 109-15.

18. Gilman JW (1999) lammability and Thermal Stability Studies of Polymer Layered-Silicate (Clay) Nanocomposites. Appl Clay Sci 15: 31–49.

19. Gilman JW, Jackson CL, Morgan AB, Harris Jr. R, Manias E, et al. (2000) Flammability Properties of Polymer-Layered-Silicate Nanocomposites. Polypropylene and Polystyrene Nanocomposites Chem Mater 12 1866-73.

20. Porter D, Metcalfe E, Thomas MJK (2000) Nanocomposite fire retardants — a review. Fire Mater 24: 45-52.

21. Zanetti M, Lomakin S, Camino G (2000) Polymer layered silicate nanocomposites Macromol Mater Engng 279: 1–9.

22. Armes SP (1995) Factors affecting the electrochemical formation of polypyrrole-nitrate colloids. Polym News 20: 233-7.

23. Godovski DY (2005) Electron behavior and magnetic properties of polymer nanocomposites. Thermal and Electrical Conductivity of Polymer Materials 79-122.

24. YK Kim, JW Williard, AW Frazier (1988) Solubility relationship in the system sodium nitrate-ammonium nitrate-urea-water at 0.degree. J Chem Eng Data 33: 306.

25. Omar R. Ibrahim (2012) Complexes of urea with Mn(II), Fe(III), Co(II), and Cu(II) metal ions. Adv Appl Sci Res 3: 3522-39.

26. M Sugimura, Y Kameyama, T Hashimoto, T Kobayashi, S Muramatsu (2012) INFRARED SPECTROSCOPIC INVESTIGATIONS ON THE REACTION PRODUCTS RESULTED FROM THE INTERACTION BETWEEN SILVER (I) SALTS WITH UREA AT 90 O CChem. Abs 112: 63.

27. JM Halbout, S Bilt, W Donaldson, CL Tang (1979) IEEE J Quantum Electron. QE-15: 1176.

28. Furmanova, NG Sulaimankulova, DK Resnyanskii, VF Sulaimankulov, KS Kristallografiya 41: 669.

29. Y Caglar, S Aksoy, S Ilican, M Cagmar (2009) Crystalline structure and morphological properties of undoped and Sn doped ZnO thin films, Superlattices Microstruct 46: 469–75.

30. MM Abdullah, Preeti Singh, M Hasmuddin, G Bhagavannarayana, MA (2013) Wahab, In-situ growth and ab-initio optical characterizations of amorphous Ga3Se4 thin film: a new chalcogenide compound semiconductor thin film, Scripta Mater 69: 381.

31. EL Papadopoulou, M Varda, K Kouroupis – Agalou (2008) Undoped and Al - doped ZnO films with tuned properties grown by pulsed laser deposition J Thin Solid Films 516: 8141-5.

32. M Ali Yıldırım, Aytunc Ates (2010) Influence of films thickness and structure on the photo-response of ZnO films, Opt Commun 283: 1370-7.

33. Zhifang Gao (2013) Synthesis of aluminum nitride nanoparticles by a facile urea glass route and influence of urea/metal molar ratio. Applied Surface Sci 280: 42-9.

34. Yu Qiu, Lian Gao (2014) Synthesis of Nanocrystalline Zirconium Nitride Powders by Reduction–Nitridation of Zirconium Oxide. J Am Ceram Soc 87: 352–57.

35. Sunila Abraham, G Aruldhas (1995) Spectrochimica Acta -A (USA) 51: 79-88.

36. B Malecka, A Lacz (2008) Thermal deposition of cadmium formate in inert and oxidative atmosphere, Thermochim. Acta 479: 12-6.

37. SR Jadhav, UP Khairnar (2012) Study of Optical Properties of Co-evaporated PbSe Thin Films. Arch Appl Sci Res 4: 169-77.

38. A Sawaby, MS Selim, SY Marzouk, MA Mostafa, A Hosny (2010) Structure, optical and electrochromic properties of NiO thin films. Physica 405: 3412–20.

39. G Nixon Samuel Vijayakumar, M Rathnakumari, P Sureshkumar (2011) Synthesis, dielectric, AC conductivity and non-linear optical studies of electrospun copper oxide nanofibers. Arch Appl Sci Res 3: 514-25.

40. F Urbach (1953) Origin of the E Layer of the Ionosphere J Phys Rev 92: 1324.

41. B Abay, SH Güder, H Efeoglu, KY Yogurtçu (2001) Preparation_structural_and_optical_investigations_of_ITO_nanopowder_and_ITO_epoxy_nanocomposites Turk. J Phys 25: 543-49.

42. N Ekem, S Korkmaz, S Pat, MZ Balbag, EN Cetin, M Ozmumca (2009) J Hydrogen Energy 34: 5218-22.

43. M. DiDomenico Jr, SH Wemple (1969) Oxygen-Octahedra Ferroelectrics. I. Theory of Electro-optical and Nonlinear optical Effects. J Appl Phys 40: 720-34.

44. SH Wemple, M DiDomenico (1970) Theory of the Elasto-Optic Effect in Nonmetallic Crystals Phys Rev B1:193-202.

45. MA Omar (1993) Elementary Solid-State Physics, Addison-Wesley Publishing Company, New York, 1993.

46. M Sesha Reddy, KT Ramakrishna Reddy, BS Naidu, PJ Reddy (1995) Opt Mater 4: 787-90.

47. A Amlouk, K Boubaker, M Amlouk (2010) J Alloys Compd. 490: 602-4.

48. F Gervais (2002) Mater Sci Eng R 39: 29-92.

49. MS Dresselhaus (2001) Solid state physics Part II, Opt Prop Solids 6: 732.

50. CA Arguello, DL Rousseau, SPS Porto (1969) First-Order Raman Effect in Wurtzite-Type Crystals. Phys. Rev 181: 1351-63.

51. Kanika Thukral, N Vijayan, Brijesh Rathi, G (2014) Bhagavannaryana, Sunil Verma, J. Philip, Anuj Krishna, M. S. Jeyalakshmy and S. K. Halder. Cryst Eng Comm 16: 2802.

52. I Gonzalo-Juan, L Macé, S Tengeler, A Mosallem, N Nicoloso, R (2016) Materials Chemistry and Physics 177: 472-8.

53. W Dong, C Zhu (2003) Optical properties of surface modified CdO nanoparticles, Opt. Mater. 22: 227-33.

54. S Balamurugan, AR Balu, K Usharani M Suganya, S. Anitha, D. Prabha, S (2016) Ilangovan. Pacific Science Review A: Natural Science and Engineering 18: 228-32.

55. J Elloumi-Mseddi, S Mnif, N Akacha, B Hakim, P Pigeon, G Jaouen, S (2018) Top and S. Aifa. Selective cytotoxicity of arene tricarbonylchromium towards tumour cell lines. Journal of Organometallic Chemistry 862: 7-12.

Appendix

• The interplanar spacing dhkl is calculated by the Bragg equation: $2d_{hkl}\sin(\theta) = n\lambda$ (1)

Where θ is the Bragg's angle, λ is the X-ray wavelength (λ = 1.78901Å), dhkl is the inter-planar spacing and n is the order of diffraction.

• For triclinic system the volume V of the unit cell was determined by using:

$$V = abc\sqrt{1-\cos^2\alpha-\cos^2\beta-\cos^2\gamma+2\cos\alpha\cos\beta\cos\gamma} \quad (2)$$

• The texture coefficient TC ($hk\ell$) was calculated by:

$$TC_{(hk\ell)} = \frac{I_{(hk\ell)}}{I_{0(hk\ell)}}.\left\{\frac{1}{N}\sum_{i=1}^{N}\frac{I_{(hk\ell)}}{I_{0(hk\ell)}}\right\}^{-1} \quad (3)$$

• The stacking fault probability γ was calculated using:

$$\gamma = \frac{2\pi^2}{45\sqrt{3}}\frac{\Delta(2\theta)}{\tan\theta} \quad (4)$$

where θ is the position of $hk\ell$ planes and Δ(2θ) is the peak shift for the oriented $hk\ell$ planes was measured.

• For in-depth study of the synthesized compounds, more detailed analysis is established using: Debye - Scherrer method:

$$D = \frac{k\lambda}{\beta_{hkl}\cos\theta} \quad (5)$$

Here λ represents the wavelength of X-ray radiation, β_{hkl} the full width at half maximum (FWHM) of the diffraction peak, θ the Bragg's angle and k is the shape factor equal to 0.9.

The dislocation density δ was calculated from the following equation: $\delta = \frac{1}{D^2}$ (6)

• α is the absorbance coefficient: $\alpha = 2.303\frac{A}{d}$ (7)

Where A measured absorbance, here d stands for the path length of the wave in cm was set equal to the cuvette length of 1 cm.

• Optical band gap energy can be calculated by using the Tauc model: $(\alpha h\nu) = B\left(h\nu - E_g\right)^n$ (8)

Where hυ is the incident photon energy, E_g is the optical band gap energy, n is a parameter associated with the type of electron transition, B is a constant reflecting the degree of disorder in the solid structure. The value of n depends on the nature of transition. Depending on whether the transition is direct allowed, direct forbidden, indirect allowed or indirect forbidden, n takes the value 1/2, 3/2, 2 or 3 respectively.

The empirical Urbach law: $\ell n(\alpha) = \ell n(\alpha_0) + \frac{h\nu}{E_u}$ (9)

$$E_u = \alpha\left(\frac{d\alpha}{d(h\nu)}\right)^{-1} \quad (10)$$

Where α_0 is a constant.

The extinction coefficient given by the following equation:

$$k = \frac{\alpha\lambda}{4\pi} \quad (11)$$

The refractive index: $\frac{n^2-1}{n^2+2} = 1-\sqrt{\frac{E_g}{20}}$ (12)

$$n^2 = \frac{3}{\sqrt{\frac{E_g}{20}}} - 2 \quad (13)$$

$$n = \frac{(1+R)}{(1-R)} + \sqrt{\frac{4R}{(1-R)^2} - k^2} \quad (14)$$

Where R is the reflectance and k the extinction coefficient.

The evolution of reactive index with the wavelength can be also described by the method of Wemple – Didomenico given by the following equations:

$$n^2 - 1 = \frac{E_0 E_d}{E_0^2 - E^2} \quad (15)$$

Where E_d and E_0 are single oscillator constants. E_0 is the energy of the effective dispersion oscillator; E_d is the so-called dispersion energy which measure the average strength of interband optical transitions.

$$\frac{n_\infty^2 - 1}{n^2 - 1} = 1 - \left(\frac{\lambda_0}{\lambda}\right)^2 \quad (16)$$

Where n_∞ is the long wavelength refractive index and λ_0 is the average oscillator wavelength.

$$n_{\infty}^{2} = 1 + S_0 \lambda_0^{2} \quad (17)$$

Where S_0 is the oscillator length strength.

$$n^{2} - 1 = \frac{S_0 \lambda_0^{2}}{1 - \left(\frac{\lambda_0}{\lambda}\right)^{2}} \quad (18)$$

The real and imaginary parts of dielectric constant were determined by the relations:

$$\begin{cases} \varepsilon(\lambda) = n(\lambda) - ik(\lambda) = \varepsilon_1(\lambda) - i\varepsilon_2(\lambda) \\ \varepsilon_1(\lambda) = n^2(\lambda) - k^2(\lambda) \\ \varepsilon_2(\lambda) = 2n(\lambda)k(\lambda) \end{cases} \quad (19)$$

The real and imaginary parts of dielectric constant can be given by the following equations:

$$\begin{cases} \varepsilon_1 \approx \varepsilon_\infty - \dfrac{\varepsilon_\infty w_p^{2}}{4\pi^2 c^2}\lambda^2 \\ \varepsilon_2 \approx 2nk \approx \dfrac{\varepsilon_\infty w_p^{2}}{8\pi^3 c^3 \tau}\lambda^3 \\ w_p^{2} = \dfrac{4\pi N e^2}{\varepsilon_\infty m^*} \end{cases} \quad (20)$$

Where ε_∞, w_p and τ represent the dielectric constant at high frequencies, the pulse plasma and the relaxation time, N/m* is the free carrier concentration of effective mass ratio.

Optical conductivity σ_{dc} can be obtained by:

$$\sigma_{dc} = \frac{Ne^2\tau}{m^*} \quad (21)$$